

Effects of frequency variation in modes orthogonal to the reaction path on condensed phase rate constants

K.M. Forsythe, N. Makri*

Department of Chemistry, University of Illinois, 601 S. Goodwin Avenue, Urbana, IL 61801, USA

Received 16 June 1998; received in revised form 7 August 1998; accepted 11 August 1998

Abstract

We examine the effects of frequency variation along the reaction path in intramolecular or lattice modes on the rate constant for light atom transfer in the condensed phase. Accurate quantum mechanical calculations using the quasi-adiabatic propagator path integral representation of the flux–flux auto-correlation function reveal significant variations in the reaction rate compared with the constant frequency case. The vibrationally adiabatic approximation captures these effects rather faithfully if the frequency of these modes is high, relative to that of the reaction coordinate. Significant deviations from the predictions of the adiabatic approximation are observed when low variable frequency modes are involved. In such cases, the competition between the decrease in the reactive flux accompanying a tightening or dilation of the reaction path valley and corner-cutting effects arising from sharp curvature of the reaction path leads to positive or negative corrections to the predictions of the adiabatic model. © 1999 Elsevier Science B.V. All rights reserved.

Keywords: Path integral calculations; Reaction paths; Tunneling; Vibrational frequencies

1. Introduction

The study of defect tunneling in/on solids has been the subject of numerous theoretical and experimental studies [1–8]. One of the most commonly found impurities is hydrogen; because of its light mass, hydrogen exhibits significant quantum effects, and its static and dynamical properties can have significant implications for the electrical properties of the material [9,10]. From a theoretical point of view, the relatively high degree of order encountered in crystalline solids makes impurity diffusion an ideal candidate for application of theoretical models based on

reaction path/harmonic bath descriptions of the dynamics [11,12].

In the most interesting regime of moderate temperature, impurity diffusion takes place via incoherent site-to-site hops, which can be described by a rate equation. At the simplest level, the rate can be estimated using the classical transition state approximation [13], which can be cast into a variational theory; see for example Ref. [2]. Although transition state theory ignores re-crossing effects, it has been shown to lead to fairly accurate predictions in the regime characterized by over-damped dynamics. More challenging is the inclusion of quantum effects. Within a separable approximation, the classical reaction rate is augmented by a correction factor for tunneling along the reaction path [14,15], while zero point energy effects in orthogonal degrees of freedom are incorporated adiabatically [16–18]. Multidimensional

* Corresponding author. Tel.: + 1-217-333 6589; fax: + 1-217-244-0789.

E-mail address: nancy@makri.scs.uiuc.edu (N. Makri)

tunneling can be captured within the centroid density approximation [19,20], which involves path integral calculations in imaginary time as well as by multi-dimensional TST methods which incorporate tunneling using various semi-classical methods [21].

Fully quantum mechanical calculation of rate constants is best achieved via the reactive flux correlation function formalism [22,23]. For condensed phase systems, evaluating the flux requires quantum propagation for the multidimensional Hamiltonian, which poses an extremely difficult problem. A tractable methodology has been developed in our group for processes that can be described in terms of a reaction coordinate coupled to a multidimensional harmonic bath [24,25]. This is based on a quasi-adiabatic propagator partitioning of the Hamiltonian [26] to construct accurate and smooth propagators which are employed to evaluate the path integral representation of the flux correlation function. This approach minimizes the phase cancellation problem and allows convergence via a combination of Monte Carlo and discrete variable representation techniques.

The present article is concerned with the effects of molecular and phonon vibrations on the reaction rate in the moderate temperature regime characterized by activated dynamics with quantum corrections. We focus on the effects of frequency variation of such orthogonal modes along the reaction path, and the relation of these effects to simple adiabatic models. These phenomena are very clearly illustrated via the diffusion of hydrogen and its isotopes in crystalline silicon which we examined in a recent publication [27].

Section 2 reviews the path integral methodology for evaluating the reactive flux correlation function in harmonic environments and its recent extension to variable frequency baths. Section 3 presents results for a model double well system coupled to an ohmic bath, which includes variable frequency oscillators and a comparison of the exact and adiabatic rate constants. Section 4 concludes the work.

2. Methodology

The kinetics of rare events are most effectively captured via the theory of reactive flux correlations. Yamamoto [28], as well as Miller and coworkers

[23,29], have presented a fully quantum-mechanical formalism of reaction rates. In the work of Miller et al. [29], the rate constant is expressed in terms of the time integral of the flux–flux auto-correlation function:

$$k_{\text{qm}} = Z^{-1} \int_0^{t_p} C_f(t) dt \quad (1)$$

where the correlation function is defined as:

$$C_f(t) = \text{Tr} \left(F e^{iHt_c/\hbar} F e^{-iHt_c/\hbar} \right) \quad (2)$$

In the last equation, H is the Hamiltonian that characterizes the reaction and F is the symmetrized flux operator:

$$F = \frac{1}{2m_0} [p_s \delta(s - s_0) + \delta(s - s_0) p_s] \quad (3)$$

which measures the quantum mechanical reactive flux through a dividing surface that intersects the reaction coordinate s at a point s_0 separating reactants from products. Finally, $t_c = t - i\hbar\beta/2$ is a complex time that arises from combining the time evolution operator with the Boltzmann operator. Eq. (2) has been used as the starting point for numerous rigorous or approximate calculations of quantum mechanical rate constants.

In the present context, the Hamiltonian is expressed in terms of a reaction coordinate coupled to a bath of n harmonic oscillators. Our expression is the Cartesian reaction coordinate expansion [12,30] of the Hamiltonian and thus all coupling is incorporated within the potential energy; the particular form is referred to as the diabatic system-bath Hamiltonian, in contrast to the adiabatic reaction path Hamiltonian for which coupling is present within the kinetic energy portion [11]. The bath of harmonic oscillators usually corresponds to the phonon vibrations of the solid, although a few intramolecular modes or coordinates of the impurity can also be incorporated into the bath. Here we allow one or more of the bath degrees of freedom to have frequencies that vary along the reaction path:

$$H = \frac{p_s^2}{2m_0} + V_0(s) + \sum_{i=1}^n \frac{p_i^2}{2m_i} + \frac{1}{2} m_i \omega_i(s)^2 Q_i^2 - f_i(s) Q_i \quad (4)$$

Using this Hamiltonian, the starting point for our

calculation of the quantum mechanical flux correlation function is Feynman's path integral formulation of quantum mechanics [31–33]. Approximating the derivatives in Eq. (3), using a finite difference, the expression for the flux correlation function is brought into the form [25]:

$$C_f(t) = \frac{\hbar^2}{2m_0^2 v_{FD}^2} \text{Re}[K(s_{FD}, s_{FD}, 0, 0; t_c) - K(0, s_{FD}, 0, s_{FD}; t_c) + K(0, 0, 0, s_{FD}; t_c) + K(s_{FD}, 0, 0, 0; t_c)] \quad (5)$$

where s_{FD} is a system coordinate point chosen sufficiently close to the dividing surface to approximate derivatives and:

$$K(s, s', s'', s'''; t_c) = \int d^n Q \langle Q | \langle s''' | e^{iH_c t_c / \hbar} | s'' \rangle \langle s' | e^{-iH_c t_c / \hbar} | s \rangle | Q \rangle \quad (6)$$

Until recently, evaluation of path integral expressions involving real time propagators was generally unstable due to phase cancellation [34]. We have been able to obtain converged results using the quasi-adiabatic propagator path integral (QUAPI) methodology for rate constants developed recently in our group [25,26]. This employs a one-dimensional adiabatic reference to partition the time evolution operator. The reference Hamiltonian H_0 is constructed from the Cartesian kinetic energy of the system plus the potential along the one-dimensional adiabatic path, which minimizes the total potential energy at fixed values of the system coordinate. This path is specified by the relations:

$$Q_i = \frac{f_i(s)}{m_i \omega_i(s)^2} \quad (7)$$

The resulting reference Hamiltonian takes the form:

$$H_0 = \frac{p_s^2}{2m_0} V_0(s) - \sum_{i=1}^n \frac{f_i(s)}{2m_i \omega_i(s)^2} \quad (8)$$

Next, the time evolution operator for a complex time increment Δt_c is split symmetrically as the

product:

$$\exp(-iH\Delta t_c/\hbar) \approx \exp(-i(H - H_0)\Delta t_c/2\hbar) \exp(-iH_0\Delta t_c/\hbar) \exp(-i(H - H_0)\Delta t_c/2\hbar) \quad (9)$$

which can be evaluated in the coordinate representation to give the quasi-adiabatic approximation to the short time propagator. Use of the latter to evaluate the complex time evolution operators in Eq. (6) leads [25] to the following QUAPI representation of the terms, entering the expression for the flux correlation function, Eq. (5) [25]:

$$K(s_1, s_{N+1}, s_{N+2}, s_{2N+2}; t_c) = \int_{-\infty}^{\infty} ds_2 \cdots \int_{-\infty}^{\infty} ds_N \cdots \int_{-\infty}^{\infty} ds_{N+3} \cdots \int_{-\infty}^{\infty} ds_{2N+1} \prod_{k=N+3}^{2N+2} \langle s_k | e^{iH_0 \Delta t_c / \hbar} | s_{k-1} \rangle \times \prod_{k=2}^{N+1} \langle s_k | e^{iH_0 \Delta t_c / \hbar} | s_{k-1} \rangle \times F(s_1, s_2, \dots, s_N, s_{N+1}, s_{N+2}, \dots, s_{2N+2}) \quad (10)$$

Here, $\Delta t_c \equiv t_c/N$, a complex time step and F is an influence functional that arises from integrating out the bath. As the harmonic bath degrees of freedom are not coupled to each other, the total influence functional factorizes:

$$F = \prod_{i=1}^n F_i(s_1, \dots, s_{2N+2}) \quad (11)$$

The influence functional arising from constant frequency modes has been given in earlier work [25]. For variable frequency oscillators, the influence functional can still be evaluated analytically and the result is detailed in Ref. [14].

The propagators involving the one-dimensional adiabatic reference H_0 are evaluated exactly using basis set methods, such that the only approximation entering Eq. (10) is due to the factorization of the propagator into parts involving non-commuting operators. This factorization becomes exact in the limit of a high-frequency bath [26]. For finite frequency bath degrees of freedom, the error introduced is proportional to the non-adiabaticity of the

Hamiltonian and the quasi-adiabatic propagator becomes exact only in the limit of the vanishing time step. Thus, the role of the influence functional in the quasi-adiabatic propagator path integral [Eq. (10)] is to include multidimensional nonadiabatic corrections to the exact dynamics along the adiabatic path; these corrections become more accurate as the time slicing of the path integral becomes finer. Compared with conventional schemes for splitting the time-evolution operator, which employ the bare kinetic energy as the reference, the QUAPI offers the advantage of convergence with much larger time steps.

The $(2N - 2)$ -dimensional integral in the QUAPI representation of the flux correlation function are evaluated via a combination of quadrature and Monte Carlo techniques. At higher temperatures, the oscillatory character of the integrand necessitates the use of quadrature methods. Multidimensional integration is made feasible via the use of system-specific discrete variable representations [35] (DVR) of the influence functional [36]. For this purpose, the system coordinate operator, s , is diagonalized in the basis of eigenstates of the reference Hamiltonian, H_0 , generating quasi-discrete position states with eigenvalues that form the DVR grid. As the temperature is lowered, more time slices are necessary for accurate discretization of the path integral, rendering multidimensional quadrature methods impractical. Fortunately, the stronger damping associated with lower temperatures leads to smoother behavior of the integrand, making Monte Carlo schemes applicable [25].

3. Effect of variable frequency oscillators: comparison with classical and adiabatic models

The dependence of the rate constant on temperature and friction was investigated by Topaler and Makri in the case of a generic ohmic bath of constant frequency oscillators [37]. Here we focus on the effects of variable frequency bath degrees of freedom. As in Ref. [23], we restrict attention to symmetric processes and model the reaction coordinate by a potential of the form:

$$V_0(s) = -as^2 + bs^4 \quad (12)$$

with the coefficients a and b defined such that the

reactant frequency is $\omega_0 = 707 \text{ cm}^{-1}$, the imaginary barrier frequency is $\omega_b = 500 \text{ cm}^{-1}$, the barrier height is 2085 cm^{-1} and the tunneling splitting is 0.00107 cm^{-1} . If the variable frequency bath degrees of freedom are treated according to the adiabatic approximation, the double well is modified by the addition of the zero point energies of these modes:

$$V_{\text{ad}}(s) = V_0(s) + \frac{\hbar}{2} \sum_i \omega_i(s) \quad (13)$$

Here the sum is over all variable frequency modes. Accordingly, the barrier height is increased by the term:

$$\Delta V_b = \frac{1}{2} \hbar \sum_i \Delta \omega_i \quad (14)$$

where $\Delta \omega_i$ is the difference between the oscillator frequency at the transition state and at the well minimum.

We choose two types of coupling functions for the variable frequency modes, which have the form:

$$f_i(s) = c_i s \quad (15a)$$

or

$$f_i(s) = c_i s^2 \quad (15b)$$

where, according to the deformation potential approximation, the coupling coefficient of each mode is proportional to its frequency. Although linear coupling is often dominant, quadratic terms become important if the lowest order linear part is zero due to symmetry. In addition, the two types of coupling given in Eqs. (15a), (15b) represent simple models of the odd and even coupling functions encountered in symmetric isomerization reactions. All constant frequency modes are coupled linearly according to Eq. (15a) to conform with the standard model of dissipation. The variable frequency modes are characterized by symmetric functions of the type:

$$\omega_i(s) = \omega_i^0 + \Delta \omega_i e^{-\lambda s^2} \quad (16)$$

where ω_i^0 is the frequency of that mode at the well minimum.

For the following comparison, we reference the quantum rate constants to those obtained via classical

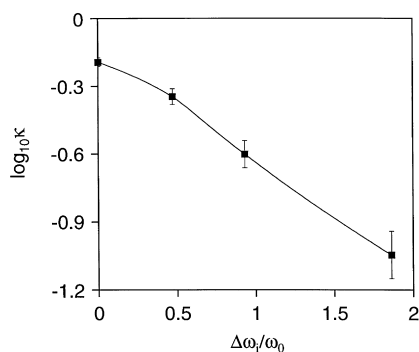


Fig. 1. Quantum transmission coefficient as a function of variable oscillator frequency dilation.

transition state theory [12,13]:

$$k_{\text{TST}} = \frac{\omega_0}{2\pi} \frac{Z_b}{Z_{\text{min}}} e^{-\beta E_b} = \frac{\omega_0}{2\pi} \frac{\prod_{i=1}^n \omega_i^0}{\prod_{i=1}^n \omega_i^b} e^{-\beta E_b} \quad (17)$$

where ω_i^0 is the bath frequency at the well minimum and ω_i^b is the bath frequency at the barrier top. The quantum transmission coefficient is then $\kappa = k_{\text{qm}}/k_{\text{TST}}$.

All values for the quantum rate constants in the results presented later were achieved with, at most, 24 DVR points and $N = 4$. Error bars are estimated from the convergence as a function of N and/or the Monte Carlo error. For all cases considered hereafter, the temperature is 300 K, which for the parameters considered is in the activated regime with significant

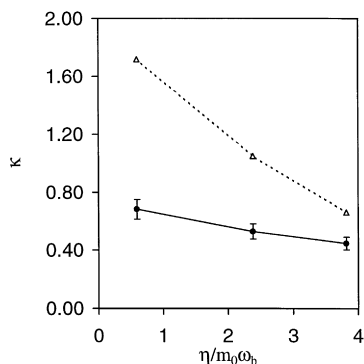


Fig. 2. Quantum transmission coefficient at several values of the friction. Solid circles: ohmic bath plus one variable oscillator ($\times 5$). Hollow triangles: constant ohmic bath only.

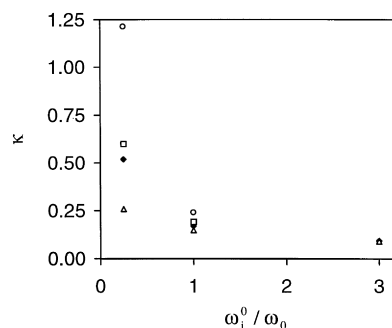


Fig. 3. Quantum transmission coefficient as a function of variable oscillator frequency referenced with respect to basin frequency of symmetric double well. Solid diamonds: adiabatic case. Hollow triangles: exact calculation with weak coupling. Hollow squares: exact calculation with strong linear coupling. Hollow circles: exact calculations with strong quadratic coupling. Error incurred is approximately 10% for all cases.

quantum corrections. We compare the exact results to the vibrationally adiabatic approximation [14,15,18,38].

Fig. 1 shows the effects on the quantum transmission coefficient in the case of a single variable oscillator characterized by linear or quadratic coupling and a frequency $\omega_i^0 = 3\omega_{\text{min}}$ for select values of $\Delta\omega_i$. In qualitative agreement with the adiabatic approximation, a positive value of $\Delta\omega_i$ leads to an increase of the effective barrier, causing the rate to decrease almost exponentially relative to the constant frequency case. Fig. 2 shows the rate constant for several values of friction; in the over-damped regime, the variable frequency rate is seen to exhibit a decrease with friction which is qualitatively similar to that in the constant frequency case [37].

Next we compare, in Fig. 3, the rate obtained from the exact calculation in the cases where the variable frequency mode is uncoupled or coupled linearly or quadratically to that given by the adiabatic approximation. In this case, the coupling of the variable frequency mode has been increased by a factor of 10 compared with that corresponding to the given friction coefficient. Couplings much larger than those of similar frequency phonons are characteristic of intramolecular or nearest lattice atom vibrations. As expected, the vibrationally adiabatic approximation is quite successful for $\omega_i^0 > \omega_0$. However, sizable differences are observed if $\omega_i^0 \ll \omega_0$. It is seen that adiabatic theory tends to overestimate the rate in the

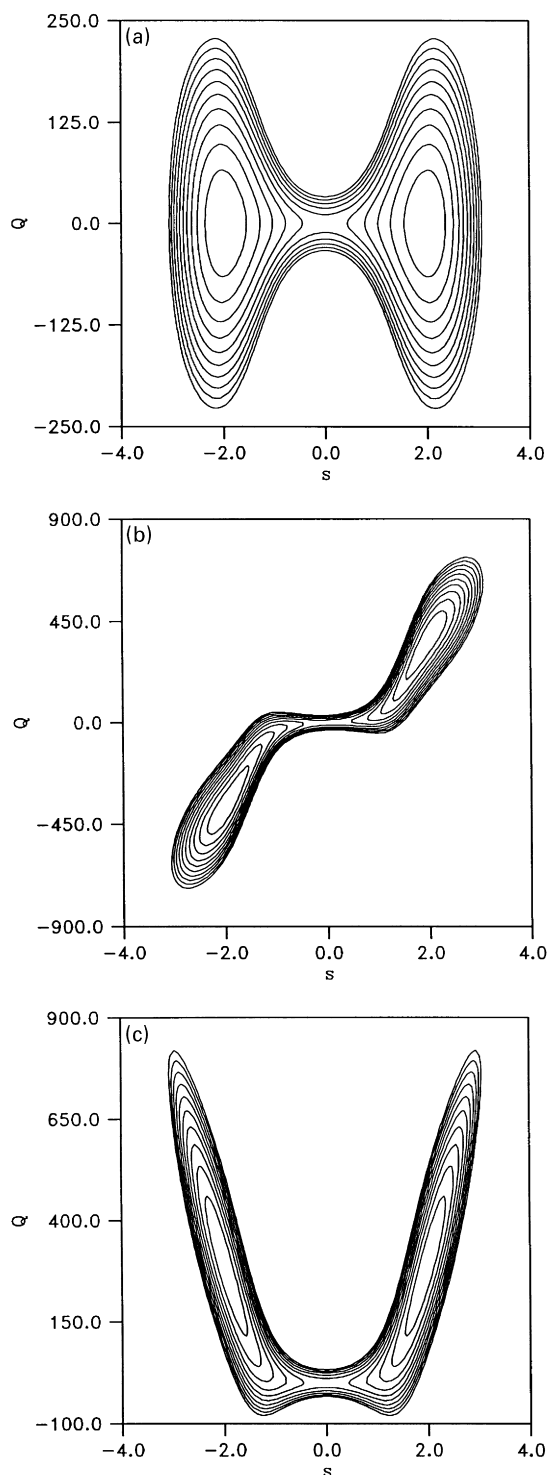


Table 1

Exact vs adiabatic transmission coefficients for system coupled to oscillators with frequencies decreasing along reaction path

$\Delta\omega_i$	Number of variable, ω_i	$\kappa_{\text{qtm}}^{\text{exact}}$	$\kappa_{\text{qtm}}^{\text{ad}}$
-6d-3	1	$3.43 \pm 7\%$	$2.78 \pm 5\%$
-9d-4	10	$11.87 \pm 11\%$	$8.52 \pm 8\%$

case where coupling of the variable frequency mode to the reaction coordinate is zero (or small), while underestimating the rate in the case of strong linear or quadratic coupling. To shed light onto this effect, we present in Fig. 4 contour plots of the potential as a function of the reaction coordinate and the variable frequency mode with all other bath degrees of freedom set to zero. The tightening of the potential valley near the transition state causes the reactive flux to be small compared with that with a constant frequency mode. This dynamical effect is ignored in the adiabatic calculation, leading to an overestimation of the rate in the case of zero or small coupling where the reaction path is relatively straight. By contrast, large coupling to the variable frequency mode leads to a reaction path that is sharply curved, generating ‘corner cutting’ tunneling contributions (Fig. 3). The latter compete with those due to the presence of a tight bottleneck, eventually leading to an increase in the rate above the value estimated by the adiabatic approximation.

Finally, we consider a situation representative of a cluster or a true lattice where multiple bath oscillators may be present. Although the fractional frequency change of each such oscillator may be quite small, the collective effects of several variable frequency oscillators can be very significant. This is the case in many condensed phase systems where motion of the impurity involves multi-atom displacement and hence frequency change in several modes [39,40]. Unlike the case of intramolecular variable frequency modes, dilution of the coupling over several lattice modes is ordinarily weak and the distortion of the concomitant bending of the reaction path is small. As a consequence, the dominant effect on the rate arises from the tightening of the reaction valley in

Fig. 4. Dilation effects of a single oscillator coupled to a symmetric double well (s and Q in atomic units). (a) Zero coupling. (b) Strong linear coupling. (c) Strong quadratic coupling.

the transition state region, implying that the adiabatic approximation is most likely to overestimate the rate constant in the case of positive frequency dilation. If, however, the frequency of the bath oscillators decreases as the transition state is approached, the effects discussed earlier will be reversed. Table 1 shows the results for numerical calculations of the rate for a single oscillator as well as a bath of 10 variable frequency oscillators with $\Delta\omega_i < 0$. These results confirm the trend described in the preceding paragraph.

4. Conclusion

It is known that the presence of variable frequency modes orthogonal to the reaction coordinate can have significant implications for the rate of a reactive process. Such effects are captured qualitatively in the vibrationally adiabatic approximation. According to the latter, the frequency variation of such modes manifests itself as a change of the effective barrier height, amounting to an exponential modification of the rate. As expected, our calculations showed the adiabatic model to be quantitatively accurate for modes whose frequency is significantly larger than that of the reaction coordinate.

Considerable deviations from the adiabatic approximation emerge in the presence of slow modes of variable frequency. Variable frequency modes are coupled to the reaction coordinate and thus affect the reaction rate even if the coupling function, $f_i(s)$, is equal to zero. Multidimensional dynamical corrections ignored in the adiabatic model can significantly affect the rate. If the direct coupling, $f_i(s)$, of the variable frequency modes to the system coordinate is small, the tightening or dilation of the valley surrounding the reaction path constitutes the dominant dynamical effect; as a consequence, the adiabatic approximation overestimates the rate if the mode frequency is higher in the saddle point region. We note that the combined effects of several weakly coupled variable frequency phonon modes can be substantial, since their zero point energies are additive. This situation is characteristic of acoustic phonons where the system-bath coupling is diluted over a large number of lattice normal modes. On the other hand, coupling to a few intermolecular or local

modes of variable frequency is likely to be large, introducing sharp turns to the reaction path. Corner cutting effects compete in this case with the saddle point bottleneck effects described earlier, and the outcome of this interplay determines whether the adiabatic approximation overestimates or underestimates the rate.

The analysis presented in the present article will be useful in assessing the direction and magnitude of dynamical corrections to the predictions of the adiabatic approximation when accurate multidimensional calculations are not available.

References

- [1] C.P. Flynn, A.M. Stoneham, *Phys. Rev. B* 1 (1969) 3966–3978.
- [2] R. Jaquet, W. Miller, *J. Phys. Chem.* 89 (1985) 2139.
- [3] Z. Zhang, K. Haug, H. Metiu, *J. Chem. Phys.* 93 (1990) 3614–3634.
- [4] C. Langpape, S. Fabian, C. Klatt, S. Kalbitzer, *Appl. Phys. A* 64 (1997) 207–210.
- [5] C.H. Seager, R.A. Anderson, *Am. Inst. Phys.* 53 (1988) 1181–1183.
- [6] S. Wonchoba, D. Truhlar, *J. Chem. Phys.* 99 (1993) 9637.
- [7] M. Stavola, Y.M. Cheng, *Solid State Comm.* 93 (1995) 431–434.
- [8] S.W. Rick, D.L. Lynch, J.D. Doll, *J. Chem. Phys.* 99 (1993) 8183–8193.
- [9] C.G. Van de Walle, P.J.H. Denteneer, Y. Bar-Yam, S.T. Pantelides, *Phys. Rev. B* 39 (1989) 10791–10808.
- [10] S.J. Pearton, W. Corbett, M. Stavola, *Hydrogen in Crystalline Semiconductors*, Springer, Berlin, 1992.
- [11] W.H. Miller, N.C. Handy, J.E. Adams, *J. Chem. Phys.* 72 (1980) 99–112.
- [12] B.A. Ruf, W.H. Miller, *J. Chem. Soc. Faraday Trans.* 84 (2) (1988) 1523–1534.
- [13] K.J. Laidler, *Theories of Chemical Reaction Rates*, McGraw-Hill, New York, 1969.
- [14] D.G. Truhlar, A. Kuppermann, *J. Chem. Phys.* 56 (1972) 2232–2252.
- [15] D.G. Truhlar, A.D. Isaacson, R.T. Skodje, B.C. Garrett, *J. Phys. Chem.* 86 (1982) 2252–2261.
- [16] R.A. Marcus, M.E. Coltrin, *J. Chem. Phys.* 67 (1977) 2609–2613.
- [17] R.A. Marcus, *J. Chem. Phys.* 46 (1967) 959.
- [18] B.C. Garrett, D.G. Truhlar, *J. Phys. Chem.* 83 (1979) 1079.
- [19] G.A. Voth, D. Chandler, W.H. Miller, *J. Chem. Phys.* 91 (1989) 7749–7760.
- [20] G.A. Voth, *Adv. Chem. Phys.* XCIII (1996) 135.
- [21] D.G. Truhlar, B.C. Garrett, S.J. Klippenstein, *J. Phys. Chem.* 100 (1996) 12771.
- [22] W.H. Miller, *Adv. Chem. Phys.* 25 (1974) 69.
- [23] W.H. Miller, *J. Chem. Phys.* 61 (1974) 1823–1834.

- [24] M. Topaler, N. Makri, *J. Chem. Phys.* 97 (1992) 9001.
- [25] M. Topaler, N. Makri, *Chem. Phys. Lett.* 210 (1993) 285–293.
- [26] N. Makri, *Chem. Phys. Lett.* 193 (1992) 435.
- [27] K. Forsythe, N. Makri, *J. Chem. Phys.* 108 (1998) 6819–6828. Erratum, in press.
- [28] T. Yamamoto, *J. Chem. Phys.* 33 (1960) 281–289.
- [29] W.H. Miller, S.D. Schwartz, J.W. Tromp, *J. Chem. Phys.* 79 (1983) 4889–4898.
- [30] W.H. Miller, B.A. Ruf, Y. Chang, *J. Chem. Phys.* 89 (1988) 6298.
- [31] R.P. Feynman, *Rev. Mod. Phys.* 20 (1948) 367–387.
- [32] R.P. Feynman, J.F.L. Vernon, *Ann. Phys.* 24 (1963) 118–173.
- [33] R.P. Feynman, A.R. Hibbs, *Quantum Mechanics and Path Integrals*, McGraw–Hill, New York, 1965.
- [34] N. Makri, *Comp. Phys. Comm.* 63 (1991) 389–414.
- [35] Z. Bacic, J.C. Light, *J. Chem. Phys.* 85 (1986) 4594.
- [36] M. Topaler, N. Makri, *Chem. Phys. Lett.* 210 (1993) 448.
- [37] M. Topaler, N. Makri, *J. Chem. Phys.* 101 (1994) 7500–7519.
- [38] R.T. Skodje, D.G. Truhlar, B.C. Garrett, *J. Phys. Chem.* 85 (1981) 3019–3023.
- [39] B.M. Rice, B.C. Garrett, *J. Chem. Phys.* 92 (1990) 775–791.
- [40] T.N. Truong, D.G. Truhlar, *J. Phys. Chem.* 91 (1987) 6229–6237.